MR-thermometry for monitoring tumor ablation

Baudouin Denis de Senneville, Charles Mougenot, Bruno Quesson, Dragonu Iulius, Nicolas Grenier, Chrit T. W. Moonen

MR-thermometry for monitoring tumor ablation

Baudouin Denis de Senneville[1], Charles Mougenot[1,2], Bruno Quesson[1], Iulius Dragonu[1], Nicolas Grenier[1,3], Chrit T.W. Moonen[1]

[1] Laboratory for Molecular and Functional Imaging: From Physiology to Therapy, CNRS/Université Bordeaux 2, 146 rue Léo Saignat, F - 33076 Bordeaux

[2] Philips Systèmes Médicaux, 64 rue Carnot, F – 92156 Suresnes

[3] Service de Radiologie - CHU Pellegrin, Bordeaux, France,

Address correspondence to:
C.T.W. Moonen
Imagerie Moléculaire et Fonctionnelle, ERT CNRS
Université « Victor Segalen » Bordeaux 2
146 rue Leo Saignat, case 117
33076 Bordeaux, France

E-Mail: chrit.moonen@imf.u-bordeaux2.fr
Tel: +33 5 57 57 45 92
Fax: +33 5 57 57 45 97

Acknowledgements: European Union, NoE "Diagnostic Molecular Imaging"; Ligue National Contre le Cancer, Conseil Régional d'Aquitaine, Philips Medical Systems, CDTU canceropôle network

Word count: 4269

Abstract

Local thermal therapies are increasingly used in the clinic for tissue ablation. During energy deposition, the actual tissue temperature is difficult to estimate since physiological processes may modify local heat conduction and energy absorption. Blood flow may increase during temperature increase and thus change heat conduction. In order to improve the therapeutic efficiency and the safety of the intervention, mapping of temperature and thermal dose appear to offer the best strategy to optimize such interventions and to provide therapy endpoints. MRI can be used to monitor local temperature changes during thermal therapies. On-line availability of dynamic temperature mapping allows prediction of tissue death during the intervention based on semi-empirical thermal dose calculations. Much progress has been made recently in MR thermometry research, and some applications are appearing in the clinic. In this paper, the principles of MRI temperature mapping are described with special emphasis on methods employing the temperature dependency of the water proton resonance frequency. Then, the prospects and requirements for widespread applications of MR thermometry in the clinic are evaluated.

Introduction

The possibility to locally deposit thermal energy in a non-invasive way (with High Intensity Focused Ultrasound, HIFU (1)) or in a minimally invasive way (using laser, radio-frequency (RF) or microwave) has opened a path toward new therapeutic strategies with improved reliability and reduced associated trauma. Among the best known of these therapies are the techniques of tumor thermo-ablation (2). Their objective is a necrosis of the tissue heated by an elevated thermal dose (TD). Those studies targeted ablation of uterine fibroids (3,4), breast cancer (5,6), prostate (7), liver (8), kidney (9), bone (10), and pancreas tumors (11). The use of a small thermal dose, in itself non-lethal for cells, can be used for innovative therapeutic strategies such as: i) regulation of transgene expression when using a heat-sensitive promoter (12); ii) local drug deposition with the help of thermo-sensitive drug nanocarriers (13).

During energy deposition, the actual tissue temperature is difficult to assess. Physiological processes may modify local heat conduction and energy absorption. Blood flow may increase during temperature increase and thus change heat conduction. In addition, the effect of heat stress is often delayed via apoptotic processes, and may thus be difficult to measure during the intervention. Semi-empirical relations between tissue damage and heat exposure have been derived by Sapareto and Dewey (14). In order to improve the therapeutic efficiency and the safety of the intervention, real-time mapping of temperature and thermal dose appear to offer the best strategy to optimize such interventions and provide clinical therapy endpoints (3,15). Currently, computer tomography (CT) and ultrasound (US) are used to monitor thermal ablation (2,3) although the extent of the lesion is difficult to assess during the intervention. Of the different imaging modalities, MRI appears the ideal tool for temperature mapping. A particular advantage of MRI for guiding thermal procedures is that MRI not only allows temperature mapping but it can be used as well for target definition. Whereas temperature effects on MR measured parameters (resonance frequency, relaxation, diffusion) had been well described previously, the first report of temperature mapping by MRI appeared in 1983 (16). The method was based on the longitudinal relaxation time (T_1). T_1 based methods have been used in the clinic and preclinical applications, in particular at low field (17,18). Since then, alternative MR temperature imaging methods have been proposed as for example techniques based on diffusion coefficient (19). However, the most widely used MR temperature mapping is based on temperature dependence of the water proton resonance frequency (PRF) (20,21,22,23). The excellent linearity of the temperature dependency of the

proton resonance frequency and its near-independence with respect to tissue type make the PRF-based method the method of choice, in particular at mid to high field strength. The reader is referred to recent reviews for principles of MR thermometry (24,25).

Quantification of the temperature changes may even allow end-point determination based on thermal dose and temperature maps. Technical difficulties related to motion artifacts and quality control in MR temperature maps, and/or the need for real-time availability of temperature data have limited the use of temperature mapping. Recently introduced improvements in MRI technologies may have an impact on the quality of temperature mapping. In addition, the stability and homogeneity of the main magnetic field of modern mid to high field instruments is excellent. The rapid acceptance of high field (3T) MRI and parallel imaging open up possibilities of further gains in SNR and imaging speed. Promising new methods have been developed that limit motion related artifacts. Further improvements and standardization are still needed to allow multi-site clinical trials. Unfortunately, temperature imaging tools are not available routinely on state-of-the-art clinical MRI instruments, a factor that limits its use in clinical research.

In this paper, principles of PRF based MR thermometry are reviewed. Then, the compatibility of the various heating devices with MR temperature mapping is evaluated. MR temperature mapping may find widespread use in the clinic. The requirements for such generalized use are described.

Basic principles of MR temperature mapping with the water Proton Resonance Frequency method

The PRF methods usually employ rapid RF-spoiled gradient echo imaging. Following image processing, an MR signal is associated for each volume element as a complex number. Grey levels on anatomical images are proportional to the MR signal magnitude value whereas its phase relates to the proton resonance frequency. Temperature variation is calculated from phase changes for each voxel obtained at different times:

$$\Delta\varphi = \gamma.\alpha.B_0.\Delta T.T_E \qquad [1]$$

where $\Delta\varphi$ is the phase difference, ΔT the temperature variation, γ the gyromagnetic ratio (~42.58.2π.10^6 rad/T), α the temperature coefficient (~0.01 ppm/K), T_E the echo time, B_0 the main magnetic field. The presence of lipids is a potential source of artifacts since the temperature dependency of the resonance frequency of lipid hydrogen is nearly zero. In practice, lipid contribution to the MR signal can be conveniently suppressed in gradient echo

imaging by frequency-selective slice excitation (26) or alternative methods (as selective fat saturation or inversion recovery).

High temperatures lead to coagulation and immediate cell death. However, moderate temperature elevations may also lead to cell death, albeit it with a delayed effect via biochemical pathways leading to apoptosis. Lethal effects of elevated temperatures have been studied by Sapareto et al (14) who established a empirical relation between temperature, duration of exposure, and cell death. Using such relations, temperature measurements throughout the procedure allow on-line thermal dose evaluation using the following equation:

$$t_{eq} = \begin{cases} \int_0^t 2^{T(t)-43}\,dt & if \quad T > 43^\circ C \\ \int_0^t 4^{T(t)-43}\,dt & if \quad T < 43^\circ C \end{cases} \qquad [2]$$

Lethal dose is reached when t_{eq} exceed 240 minutes at 43 °C (27,28). Thus, accurate thermal dose calculation requires a precise thermometry, since temperature has an exponential effect on thermal dose (see equation 2).

A summary of the basic elements required for real-time temperature mapping with the PRF method is given in Appendix 1.

Heating devices for thermal therapies and their MR compatibility

Several existing minimally invasive techniques for the treatment of primary and secondary malignant hepatic tumors have been reviewed in [2]. Here, a short description is given together with the passive MR compatibility (use of non-ferromagnetic materials) as well as the active compatibility (avoiding interference with MR data acquisition).

Laser

Laser systems are often used for high spatial precision and small volume ablations (a few mm^3 is required). Lasers have been used to treat tumors of the oesophagus (29,30), liver (31,32), lung (33,34), colon (35,36), head and neck (37), and brain (38). The laser technique has the advantage of being fully compatible with MR imaging (39). MR imaging thus offers the potential for accurate on-line monitoring of energy deposition (40).

Radiofrequency

Radio-frequency ablation for the treatment of hepatic tumors was initially proposed in 1990 (41,42). An alternating electric current is used to produce a focal thermal injury in living tissue. A maximal temperature increase of 50 °C is generated to produce coagulative necrosis. Percutaneous radiofrequency thermal ablation (43) is widely used to treat malignant hepatic tumors (<4 cm in diameter) in a few minutes (maximum 45 minutes) in patients who are not eligible for resection. This is the typical size of precociously detected tumours in the liver. Recent systems allow the ablation of larger tumours (diameter higher than 4 cm) using several electrodes (3 maximum) implanted in the tumour periphery. Thus, the main advantage of radio-frequency ablation is that the size of the thermal injury created by a single ablation is larger than that created by a single laser ablation.

Currently, computer tomography (CT) and ultrasound (US) are used to monitor RF ablation (44,45). Unfortunately, the estimation of the actual size of the ablated region is not very precise with US monitoring because the extent of the hyperechogenic zone does not strictly correspond to the necrotic area. Such a prediction may become more accurate when intravenous injection of contrast material is performed (46). Because of the impracticality of repeated injections, the extent of the ablative zone can only be assessed at the end of the procedure.

It has been recently demonstrated that quantitative temperature MRI during RF ablation is feasible (47) and offers a precise indication of the ablation zone size in this preclinical study based on the lethal dose threshold (48). A MR temperature uncertainty of 1–2 °C can be obtained even during RF deposition. The thermal dose maps were shown to be more predictive and precise than conventional MR images, with an average predictive precision for the final ablation zone size of about 1 mm as compared to the histologically proven lesion on day 8. Therefore, temperature MRI based on the TD concept may play an important role in monitoring RF ablation and providing a clinical end-point. Several limitations must be addressed before this technique can be widely applied in clinical practice. First, potential noise generated by the RF heating device can hamper image quality (active interference). For example, during RF ablation, susceptibility artifacts induced in MR images by the metallic electrode implanted in the target region and electromagnetic interferences between RF energy deposition for tissue ablation and MRI (49) remain important limitations for precise and quantitative real-time monitoring. MR compatible electrodes with different materials have been developed. The dimensions of susceptibility artefacts from several MR-compatible electrodes were previously reported (50). The induced image artifact (passive interference) acquired with a gradient echo sequence was found to be five times larger than

the actual size of the electrode when the electrode was perpendicular to the main magnetic field. RF interference artifacts around the MR frequency can be attenuated by efficient filtering.

Microwave

The basic mechanism of heat generation in living tissue consists of rotation of water molecules. Microwaves are emitted from the distal segment of a percutaneous probe. A single ablation produces an elliptical coagulated area with a maximal diameter slightly greater than 2 cm near the tip of the electrode. Ideal lesions for microwave therapy are thus less than 3 cm. Recent works demonstrated the feasibility of the combination of microwave hyperthermia system with MR temperature maps (51). This technique was applied to the treatment of liver tumors (52). Treatments are usually repeated three times a week until the entire tumor is ablated. Microwave ablation is less invasive than radiofrequency ablation as the time required for microwave ablation is very short (lower than 60 seconds). However more sessions are required to treat larger tumors.

Focused ultrasound

High Intensity Focused Ultrasound (HIFU) is a non-invasive technique for local thermal therapy (1,2). It is based on oscillating pressure waves with a wavelength of approximately 1 mm that can be concentrated into a focal point with a size depending on ultrasound frequency, focal length and aperture of the transducer. The mechanical energy is transformed into thermal energy because of local friction. The development of the noninvasive HIFU heating technique (53) and the potential of MRI for on-line temperature mapping has provided the basis for the combination of the two technologies (54) hereafter referred to as MR guided HIFU (MRgHIFU).

The available MRgHIFU procedures are dedicated for the moment to immobilized organs (breast, uterus) in which mechanical waves are not attenuated nor dispersed by other organs. The procedures remain long (several hours) because the local area of the ultrasonic waves has a small size (few mm^3). Several clinical studies using MRgHIFU have been reported for ablation of uterine fibroids (3,4) (see Figure 1 from (3)) and breast cancer (5,6), demonstrating that MR temperature mapping is indeed feasible for guiding HIFU therapy. MRgHIFU treatment has been approved for the ablation of uterine fibroids and is now used in

many hospitals. The HIFU technology is under rapid development in the cancer research field, e.g. with the treatment of brain trough the skull (55,56,57). Treatment of mobile tissues (e.g. liver and kidney tumors) would add a major new field of MR-HIFU applications. In order to make this possible, the MR-HIFU system must be adapted to take the motion into account, both with respect to positioning of the focal point (target tracking), as well as to correcting for motion artifacts in temperature mapping (58). Without such corrections, treatment may be inefficient or may induce unwanted destruction of healthy neighboring tissue.

Requirements of MR temperature for real-time cancer therapy guidance and end-point determination

MR thermometry offers a large potential for real-time therapy hyperthermia guidance and to provide therapy endpoints. However, in order to make MR temperature mapping widely useful for thermal therapies in clinical practice, much attention has to be paid on several conditions such as: 1) excellent spatial and temperature resolution; 2) on-line availability of accurate temperature maps and thermal dose maps; 3) robustness to artifacts in particular for temperature mapping of moving organs; 4) automatic quality assessment; 5) on-line visualisation of the hyperthermia procedure based on the presentation of thermal maps.

High temporal and spatial resolution

A reliable temperature measurement must be performed on a region of interest defined by the radiologist. This region contains the ablation zone with a surrounding safety interval (typically at least 5 mm). Optimal MR thermometry requires high temporal and spatial resolution to precisely monitor temperature distribution within the targeted area and to predict the efficiency of the thermal treatment. Ideally, the time delay between two successive temperature maps should be small compared to the time in which the measured temperature change would have a significant influence on the therapy (a few seconds at 50 °C up to several minutes at 43 °C). Spatial resolution should be better than the smallest structure to be tracked individually (anatomically determined), and such that temperature gradients across the voxel do not lead to signal intensity loss (due to phase distribution) and significant errors in the determination whether the lethal dose is reached (determined by the energy applicator and heat conduction). In case of Focused Ultrasound ablation, the resolution should be better than the dimensions of the focal point.

A recent review has summarized developments in rapid imaging for temperature mapping (25).

Accurate thermometry

The accuracy of MR thermometry depends on several factors such as signal to noise ratio (SNR), echo time (TE), field strength, artifacts (see below). Acceleration of image acquisition in order to increase temporal resolution usually implies a signal-to-noise reduction. It is well established that electronic noise is Gaussian white noise (59). The MR system measures the real and imaginary components of the signal. As these two data each contain (ideally) Gaussian white noise, the resulting noise in the magnitude images will have a Rician distribution (60,61).

The precision of temperature estimation can thus be estimated from the standard deviation of a time series of measurements. Because the SNR increases with magnetic field intensity, only recent fields of 1 T (or higher) offer the possibility to obtain a thermal map with accuracy close to 1 °C acquired with duration of 0.5 s per slice composed of 1 mm^3 voxels.

Accurate thermometry allows the possibility of automatic control of the thermal procedure. To obtain such a control, it has been shown that MR thermometry can be used to provide spatial and temporal temperature feedback control of the HIFU device. Until now, such a control system has been demonstrated for immobilized tissues in vitro and in vivo (62).

Low level of artefacts due to susceptibility effects

It has usually been assumed that, for PRF methods, macroscopic magnetic susceptibility effects are independent of temperature. A susceptibility field modification generates a perturbation of the magnetic field in the MRI and thus of the measured signal phase. Magnetic susceptibility is usually spatially inhomogeneous (in particular near intestines, stomach, oesophagus, lungs, …), and increase with B_0 intensity. However, it has been demonstrated that temperature dependent changes in magnetic susceptibility may not be negligible (63,64).

Low level of artefacts due to motion

Complex organ displacement and deformation (mainly induced by breathing or cardiac activity) must be compensated in order to:

- improve the precision of on-line temperature measurement by performing phase difference on pixels corresponding to identical spatial localisation,
- enable temporal extraction of information on images and thus make possible on-line thermal dose computation (as for each pixel, the history of the temperature corresponding to the same spatial localization in the organ is required, see equation (2)),
- preserve for each acquired image the validity of regions of interest defined by the radiologist at the beginning of the intervention (the targeted region for example).

In addition, although the spatial transformation of the reference phase image can be corrected, an unwanted phase shift cannot be fully suppressed. In fact, the local magnetic susceptibility distribution is modified when a motion occurs. Therefore, both PRF-shift with temperature and movements of the patient result in phase variation and it is not possible to separate these two contributions within a single phase image. Correction of motion related errors is one of the most challenging tasks in temperature MRI and is subject to active research. Techniques are now explored to allow correcting motion related errors in PRF based MR thermometry avoiding explicit modelling of the susceptibility field (25).

Visualisation

A 3D visualization of temperature evolution based on multi-slice imagery must be developed in order to allow a precise monitoring of the therapy. With recent improvements of spatial and temporal resolution of MR data, this visualisation will become essential for the radiologist for an accurate localization of necrosis areas and to avoid destruction of healthy neighboring tissue.

Conclusion

Clinical results of minimally invasive ablation techniques are comparable to those obtained with conventional chemotherapy or radiation therapy (2). For non-surgical patients, these techniques are becoming standard independent or adjuvant therapies. An on-line temperature monitoring appears the best strategy to further improve the outcome. For optimal treatment, temperature in the targeted volume should be controlled accurately and

continuously. The excellent linearity of the temperature sensitivity of the water PRF and its near independence with respect to the nature of the tissue make PRF-based approach the preferred choice for temperature monitoring. PRF methods can be used in conjunction with all heating devices. The combination of focused ultrasound and MRI is especially promising since MRI allows a high precision of target localization and it is the only noninvasive imaging technique that has been shown to allow accurate temperature mapping in vivo. For those reason, HIFU ablation guided by MRI has been called the surgery of the future (65). A MR feedback control system has been demonstrated for HIFU treatment of immobilized tissues in vitro and in vivo. Major problems for liver, kidney and heart are artifacts related to magnetic susceptibility effects and motion. Promising techniques are now being developed to allow MR temperature measurement on mobile organs.

Appendix: Acquisition, image processing, and visualisation sequence for MR temperature mapping

PRF thermometry uses a gradient echo acquisition and may benefit from the wide number of rapid gradient echo imaging techniques developed for several MRI applications (66), and widely available on state-of-the-art MRI equipment. A compromise has to be made in the choice of the acquisition parameters for a given imaging sequence and a target organ with the following objectives:

- High temporal (1-5 s) and spatial (1-3 mm) resolution.
- High temperature precision. For that purpose, T_E must be similar to T_2*. In addition, the signal to noise ratio (SNR) is directly related to uncertainty in temperature estimate. For example, to obtain a temperature precision of 1 °C, SNR should be at least 9 in the kidney (for which the typical value of T_2*~30-40 ms is obtained at 1.5T), 23 in the liver (T_2*~15 ms) and 5 in the brain (T_2*~60-70 ms). It can be noticed that rather low SNR values are sufficient to obtain accurate temperature maps (as compared to SNR requirements for visualisation of anatomical structures).
- No motion artefacts. Motion restraining devices in the positioning of the patient can be used. In addition, the simplest technique to reduce periodic motion artifacts is to synchronize the acquisition of the images to a stable part of the cycle (e.g. at the end of expiration for breathing). Synchronization can be achieved by triggering the MR pulse sequence (40) based on electric signals provided by a pressure sensor (“respiratory gating”) or cardiac electrodes (“cardiac gating”). Alternatively, MR

methods can be employed using navigator echoes). The major drawback of those methods is that the temporal resolution depends on the motion frequency and a limited set of images can be acquired during a respiratory cycle (~ 5 seconds for humans).

- Elimination of potential source of artifacts generated by the presence of lipids (since the temperature dependency of the resonance frequency of lipid hydrogen is nearly zero). In practice, lipid contribution to the MR signal can be conveniently suppressed in gradient echo imaging by frequency-selective slice excitation (26) or alternative methods (as selective fat saturation or inversion recovery).
- Low image distortions. Magnetic susceptibility is usually spatially inhomogeneous possibly inducing important image distortions, especially in the case of rapid phase-sensitive, PRF-based, MR thermometry.

The reconstructed signal is a complex number: grey levels on anatomical images are proportional to the magnitude value whereas its phase value relates to the proton resonance frequency. This initial data processing is done on-line by the MR acquisition computer. Then, temperature computation requires the use of reference phase maps (20,21). This specific processing is not available on standard MRI. Real and imaginary data are thus transferred on-line to a workstation in charge of temperature computation and visualization and, if possible, control of the heating device. Temperature maps are thus computed by analyzing contrast variation on phase images (24) (see equation 1).

Artifacts on temperature maps should then be reduced to a level of negligible error both with respect to anatomy as well as temperature. Artifacts in anatomy appearing in gradient echo imaging have been reviewed elsewhere (67). Temperature mapping using the PRF method is particularly subject to thermometry errors since a small phase change may not lead to errors in anatomical features but give significant thermometry errors via equation 1. On-line PRF temperature measurement may only be reliable when potential problems are eliminated due to (25):

- possible low SNR values due to the use of rapid acquisition sequences or lack of water hydrogen signal in the observed region,
- spatial and temporal drift of the magnetic field,
- local phase discontinuities and wrapping: the observable phase signal is 2π-periodic (it is a function of the wrapped phase) and accounts for the noise sources present in MR imaging. A robust unwrapping algorithm is required for accurate temperature computation as thermal map results from phase difference (see equation 1) (20,21). As temperature computation is performed individually for each voxel, aliasing problem

can be solved using a temporal unwrapping correction. Temperature has to be unwrapped in order to correct for possible temporal discontinuities by bringing back $\Delta\varphi$ in the interval $[-\pi,\pi[$ by adding or subtracting 2π. However, phase difference can exceed 2π during the complete intervention in the case of important rise of temperature. As changes in phase variations between successive images are much smaller, temperature aliasing correction is performed on successive acquisitions.

Accurate MR temperature monitoring has been demonstrated for immobilized organ. Techniques are now being developed to allow MR temperature measurement of mobile organs. Much attention is paid for organs of the abdomen as they are prone to periodic displacements induced by breathing or cardiac activity. Accelerated acquisition techniques are used (acquisition time per image faster than typical motion period) and the phase perturbation associated with organ motion is analyzed during a pre-treatment step. A collection of multiple baseline reference phase images for different position of the organ is used to generate temperature maps Since this is not the primary focus of this paper, the reader is referred to recent articles (25,40,58).

Systematic quality control of rapid, on-line, temperature maps should then be carried out, in particular when artifacts may occur due to motion and to specific MR image reconstruction such as parallel imaging which may induce spatially dependant SNR losses. Automatic and semi-automatic therapy controls require continuous assessment of the reliability of the available temperature maps. The temperature standard deviation is a good indicator of thermometry quality in a region where no heating is performed. Depending on the application, a typical maximal value may be defined by the radiologist (2 °C for instance). During the intervention, this criterion is hard to evaluate within the targeted area because of the temperature rise. However, an evaluation can be carried out outside the heated region thus approximating the quality in the target region. If the quality tests fail, the erroneous image should be rejected and additional computations be performed (for example, the last correctly acquired image is taken into account). If the quality tests succeed, thermal dose map is computed using equation 2.

Images can thus be displayed, analyzed and stored. Visualization should be in real-time and include temperature and thermal dose maps, and allow evaluation of the entire target volume (or at least three parallel maps or two orthogonal maps).

References

(1) Lele PP., Production of deep focal lesions by focused ultrasound current status. Ultrasonics, 1967, vol. 5, pp. 105-112.

(2) Dodd G. D., Soulen M. C., Kane R. A., Livraghi T., Lees W. R., Yamashita Y., Gillams A. R., Karahan O. I., and Rhim H., Minimally invasive treatment of malignant hepatic tumors: at the threshold of a major breakthrough. Radiographics 20 (1):9-27, 2000.

(3) Tempany C. M., Stewart E. A., McDannold N., Quade B. J., Jolesz F. A., Hynynen K., MR imaging-guided focused ultrasound surgery of uterine leiomyomas: a feasibility study. Radiology. 2003 Mar;226(3):897-905.

(5) Furusawa H., Namba K., Thomsen S., Akiyama F., Bendet A., Tanaka C., Yasuda Y., and Nakahara H., Magnetic resonance-guided focused ultrasound surgery of breast cancer: reliability and effectiveness. J.Am.Coll.Surg. 203 (1):54-63, 2006.

(6) Zippel D. B., Papa M. Z., The use of MR imaging guided focused ultrasound in breast cancer patients; a preliminary phase one study and review. Breast Cancer. 2005; 12:32-8.

(7) Uchida T., Ohkusa H., Yamashita H., Shoji S., Nagata Y., Hyodo T., and Satoh T., Five years experience of transrectal high-intensity focused ultrasound using the Sonablate device in the treatment of localized prostate cancer. Int.J.Urol. 2006;13 (3):228-233.

(8) Kennedy J. E., Wu F., ter Haar G. R., Gleeson F. V., Phillips R. R., Middleton M. R., and Cranston D. High-intensity focused ultrasound for the treatment of liver tumours. Ultrasonics 2004;42 (1-9):931-935.

(9) Hacker A., Michel M. S., Marlinghaus E., Kohrmann K. U., and Alken P., Extracorporeally induced ablation of renal tissue by high-intensity focused ultrasound. BJU.Int. 2006;97 (4):779-785.

(10) Wu F., Wang Z. B., et al. Non-invasive ablation of high intensity focused ultrasound for the treatment of patients with malignant bone tumours. J Bone Joint Surg (Br) 2003;87-B; Issue Supp I, 4.

(11) Wang X. and Sun J., High-intensity focused ultrasound in patients with late-stage pancreatic carcinoma. Chin Med.J.(Engl.) 2002;115 (9):1332-1335.

(12) Guilhon E., Quesson B., Moraud-Gaudry F., de Verneuil H., Canioni P., Salomir R., Voisin P., Moonen C. T. W., Image-guided control of transgene expression based on local hyperthermia. J. Molecular Imaging, 2(1):11-7, 2003.

(13) Madio D. P., Van Gelderen P., DesPres D., Olson A. W., de Zwart J. A., Fawcett T. W., Holbrook N., Mandel M., Moonen C. T. W., On the feasibility of MRI-guided focused ultrasound for local induction of gene expression, Journal of Magnetic Resonance Imaging 8, 101-104, 1998.

(14) Sapareto S. A., Dewey W. CL, Thermal dose determination in cancer therapy. Int. J. Radiation Oncology Biol. Phys. 10, 787-800. 1984.

(15) Lepetit-Coiffe M., Quesson B., Seror O., Dumont E., Le Bail B., Moonen C. T. W., and Trillaud H., Real-Time Monitoring of Radiofrequency Ablation of Rabbit Liver by Respiratory-Gated Quantitative Temperature MRI, Journal of Magnetic Resonance Imaging, 24:152–159 (2006).

(16) Parker D. L., Smith V., Sheldon P., Crooks L. E., Fussell L., Temperature distribution measurements in two-dimensional NMR imaging. Med Phys 1983;10(3):321-5.

(17) Fried M. P., Morrison P. R., Hushek S. G., Kernahan G. A., Jolesz F. A., Dynamic T1-weighted magnetic resonance imaging of interstitial laser photocoagulation in the liver: observations on in vivo temperature sensitivity. Lasers Surg Med 1996;18(4):410-9.

(18) Graham S. J., Bronskill M. J., Henkelman R. M., Time and temperature dependence of MR parameters during thermal coagulation of ex vivo rabbit muscle. Magn Reson Med 1998;39(2):198-203.

(19) Le Bihan D., Delannoy J., Levin R. L., Temperature mapping with MR imaging of molecular diffusion: application to hyperthermia. Radiology 1989;171(3):853-7.

(20) De Poorter J., De Wagter C., De Deene Y., Thomsen C., Stahlberg F., Achten E., Noninvasive MRI thermometry with the proton resonance frequency (PRF) method: in vivo results in human muscle. Magn Reson Med 1995;33(1):74-81.

(21) Ishihara Y., Calderon A., Watanabe H., Okamoto K., Suzuki Y., Kuroda K., et al., A precise and fast temperature mapping using water proton chemical shift. Magn Reson Med 1995;34(6):814-23.

(22) Peters R. D., Henkelman R. M., Proton-resonance frequency shift MR thermometry is affected by changes in the electrical conductivity of tissue. Magn Reson Med 43:62-71, 2000.

(23) Wlodarczyk W., Boroschewski R., Hentschel M., Wust P., Monich G., Felix R., Three-dimensional monitoring of small temperature changes for therapeutic hyperthermia using MR. J Magn Reson Imaging 1998;8(1):165-74.

(24) Quesson B., de Zwart J. A., Moonen C. T. W., Magnetic resonance temperature imaging for guidance of thermotherapy. J Magn Reson Imaging 2000;12(4):525-33.

(25) Denis de Senneville B., Quesson B., Moonen C. T. W., Magnetic Resonance Temperature imaging, International Journal of Hyperthermia 2005; 21(6): 515-531.

(26) de Zwart J. A., Vimeux F. C., Delalande C., Canioni P. Moonene C. T. Fast lipid-suppressed MR temperature mapping with echo-shifted gradient-echo imaging and spectral-spatial excitation, Magn Reson Med 1999; 42(1):53-9.

(27) McDannold N., Hynynen K., Wolf D., Wolf G., Jolesz F., MRI evaluation of thermal ablation of tumors with focused ultrasound. J. Magn. Reson. Ig, 8:91-100, 1998.

(28) Cline H. E., Hynynen K., Hardy C. J., Watkins R. D. Schenck J. F., Jolesz F. A., MR temperature mapping of focused ultrasound surgery. Magn. Reson. Med. 31:628-636, 1994.

(29) Popat S., Lopez J., Chan S., Waters J., Cominos M., Rutter D., and Hill M. E., Palliative treatments for patients with inoperable gastroesophageal cancers. *Int.J.Palliat.Nurs.* 12 (7):306-317, 2006.

(30) Dahan L., Ries P., Laugier R., and Seitz J. F., Palliative endoscopic treatments for esophageal cancers. *Gastroenterol.Clin.Biol.* 30 (2):253-261, 2006.

(31) Germain D., Chevallier P., Laurent A., Savart M., Wassef M., and Saint-Jalmes H., MR monitoring of laser-induced lesions of the liver in vivo in a low-field open magnet: temperature mapping and lesion size prediction. *J.Magn Reson.Imaging* 13 (1):42-49, 2001.

(32) Vogl T. J., Straub R., Zangos S., Mack M. G., and Eichler K., MR-guided laser-induced thermotherapy (LITT) of liver tumours: experimental and clinical data. *Int.J.Hyperthermia* 20 (7):713-724, 2004.

(33) Vogl T. J., Fieguth H. G., Eichler K., Straub R., Lehnert T., Zangos S., and Mack M., Laser-induced thermotherapy of lung metastases and primary lung tumors. *Radiologe* 44 (7):693-699, 2004.

(34) Vogl T. J., Lehnert T., Wetter A., Mack M. G., and Wurster M. G., Interventional radiology in Carney triad. *Eur.Radiol.* 15 (4):833-837, 2005.

(35) Fiorella M. L., Ross D. A., White R. I., Sabba C., and Fiorella R., Hereditary haemorrhagic telangiectasia: state of the art. *Acta Otorhinolaryngol.Ital.* 24 (6):330-336, 2004.

(36) Maataoui A., Qian J., Mack M. G., Straub R., Oppermann E., Khan M. F., Knappe V., and Vogl T. J., Laser-induced Interstitial thermotherapy (LITT) in hepatic metastases of various sizes in an animal model. *Rofo* 177 (3):405-410, 2005.

(37) Eyrich G. K., Bruder E., Hilfiker P., Dubno B., Quick H. H., Patak M. A., Gratz K. W., and Sailer H. F., Temperature mapping of magnetic resonance-guided laser interstitial thermal

therapy (LITT) in lymphangiomas of the head and neck. *Lasers Surg.Med.* 26 (5):467-476, 2000.

(38) Atsumi H. and Matsumae M., Laser interstitial thermo therapy (LITT) for brain tumors. *Nippon Rinsho* 63 Suppl 9:495-498, 2005.

(39) Peters R. D., Chan E., Trachtenberg J., Jothy S., Kapusta L., Kucharczyk W., et al. Magnetic resonance thermometry for predicting thermal damage: an application of interstitial laser coagulation in an in vivo canine prostate model. Magn Reson Med 2000;44(6):873-883.

(40) Vigen K. K., Daniel B. L., Pauly J. M., and Butts K., Triggered, navigated, multi-baseline method for proton resonance frequency temperature mapping with respiratory motion. *Magn Reson.Med.* 50 (5):1003-1010, 2003.

(41) McGahan J. P., Browning P. D., Brock J. M. , Teslik H., Hepatic ablation using radiofrequency electrocautery. Invest Radiol 1990; 25:267-270.

(42) Rossi S., Fornari F., Pathies C., Buscarini L., Thermal lesions induced by 480 KHz localized current field in guinea pig and pig liver. Tumori 1990; 76:54-57.

(43) Nour S. G., Standardization of terms and reporting criteria for imageguided tumor ablation. Radiology 2004;232:626–627; author reply 627.

(44) Chen M. H., Yang W., Yan K., et al., Large liver tumors: protocol for radiofrequency ablation and its clinical application in 110 patients - mathematic model, overlapping mode, and electrode placement process. Radiology 2004;232:260–271.

(45) Solbiati L., Ierace T., Tonolini M., Cova L., Guidance and monitoring of radiofrequency liver tumor ablation with contrast-enhanced ultrasound. Eur Journ Radiol 2004;51(Suppl):S19–S23.

(46) Solbiati L., Tonolini M., Cova L., Monitoring RF ablation. Eur Radiol 2004;14(Suppl 8):P34–P42.

(47) Gellermann J., Wlodarczyk W., Feussner A., Fahling H., Nadobny J., Hildebrandt B., Felix R., and Wust P., Methods and potentials of magnetic resonance imaging for monitoring radiofrequency hyperthermia in a hybrid system. *Int.J.Hyperthermia* 21 (6):497-513, 2005.

(48) Lepetit-Coiffe M., Quesson B., Seror O., Dumont E., Le Bail B. , Moonen C. T. W., and Trillaud H., Real-time monitoring of radiofrequency ablation of rabbit liver by respiratory-gated quantitative temperature MRI. *J.Magn Reson.Imaging* 24 (1):152-159, 2006.

(49) Rhim H., Goldberg S. N., Dodd 3rd G. D., et al. Essential techniques for successful radio-frequency thermal ablation of malignant hepatic tumors. Radiographics 2001;21(spec no):S17–S35; discussion S36–S19.

(50) Aube C., Schmidt D., Brieger J., et al. Magnetic resonance imaging characteristics of six radiofrequency electrodes in a phantom study. J Vasc Interv Radiol 2004;15:385–392.

(51) Demura K., Morikawa S., Murakami K., Sato K., Shiomi H., Naka S., Kurumi Y., Inubushi T., and Tani T., An easy-to-use microwave hyperthermia system combined with spatially resolved MR temperature maps: phantom and animal studies. *J.Surg.Res.* 135 (1):179-186, 2006.

(52) Sato K., Morikawa S., Inubushi T., Kurumi Y., Naka S., Haque H. A., Demura K., and Tani T., Alternate biplanar MR navigation for microwave ablation of liver tumors. *Magn Reson.Med.Sci.* 4 (2):89-94, 2005.

(53) Lynn J. G., Putman T. J., Histological and cerebral lesions produced by focused ultrasound. Am J Pathol, 1944 ; 20 :637-649.

(54) Cline H. E., Schenck J. F., Hynynen K., Watkins R. D., Souza S. P., and Jolesz F. A., MR-guided focused ultrasound surgery. J.Comput.Assist.Tomogr. 1992;16 (6):956-965.

(55) Pernot M., Aubry J. F., Tanter M., Thomas J. L., and Fink M., High power transcranial beam steering for ultrasonic brain therapy. Phys.Med.Biol. 48 (16):2577-2589, 2003.

(56) Hynynen K., McDannold N., Clement G., Jolesz F. A., Zadicario E., Killiany R., Moore T., and Rosen D., Pre-clinical testing of a phased array ultrasound system for MRI-guided noninvasive surgery of the brain-A primate study. Eur.J.Radiol., 2006; 59(2):149-56.

(57) Ram Z., Cohen Z. R., Harnof S., Tal S., Faibel M., Nass D., Maier S. E., Hadani M., and Mardor Y., Magnetic resonance imaging-guided, high-intensity focused ultrasound for brain tumor therapy. *Neurosurgery* 59 (5):949-955, 2006.

(58) Denis de Senneville B., Mougenot C., Moonen C. T. W., Real time adaptive methods for treatment of mobile organs by MRI controlled High Intensity Focused Ultrasound, Magnetic Resonance in Medicine, 2007. Volume 57, Issue 2 , Pages 319 – 330.

(59) Bennett W.R., Electrical Noise. McGraw Hill, New-York, 1962.

(60) Gudbjartsson H., Patz S., The Rician Distribution of Noisy MRI Data, Magnetic Resonance in Medicine, 34:910-914, 1995.

(61) Sijbers J., den Dekker A. J., Maximum Likelihood Estimation of Signal Amplitude and Noise Variance From MR data, Magnetic Resonance in Medicine, 51:589-594, 2004.

(62) Mougenot C., Salomir R., Palussière J., Grenier N., Moonen C. T. W., Automatic Spatial and Temporal Temperature Control for MR-guided Focused Ultrasound Using Fast 3D MR Thermometry and Multispiral Trajectory of the Focal Point, Magnetic Resonance in Medicine 2004; 52:1005-1015.

(63) De Poorter J., De Wagter C., De Deene Y., Thomson C., Stahlberg F., Achten E., The proton resonance frequency shift method compared with molecular diffusion for quantitative measurement of two dimensional time dependent temperature distribution in phantom, J Magn Reson, 103: 234-241, 1994.

(64) Young I. R., Hajnal J. V., Roberts I. G., Ling J. X., Hill-Cottingham R. J., Oatridge A., et al. An evaluation of the effects of susceptibility changes on the water chemical shift method of temperature measurement in human peripheral muscle. Magn Reson Med 1996;36(3):366-74.

(65) Kennedy J. E., ter Haar G. R., and Cranston D., High intensity focused ultrasound: surgery of the future? Br.J.Radiol. 76 (909):590-599, 2003.

(66) Scheffler K., Fast frequency mapping with balanced SSFP: theory and application to proton-resonance frequency shift thermometry. Magn Reson Med 2004;51(6):1205-11.

(67) Riederer S. J., Recent technical advances in MR imaging of the abdomen, Journal of Magnetic Resonance Imaging, 6:822-832 (1996).

Figures:

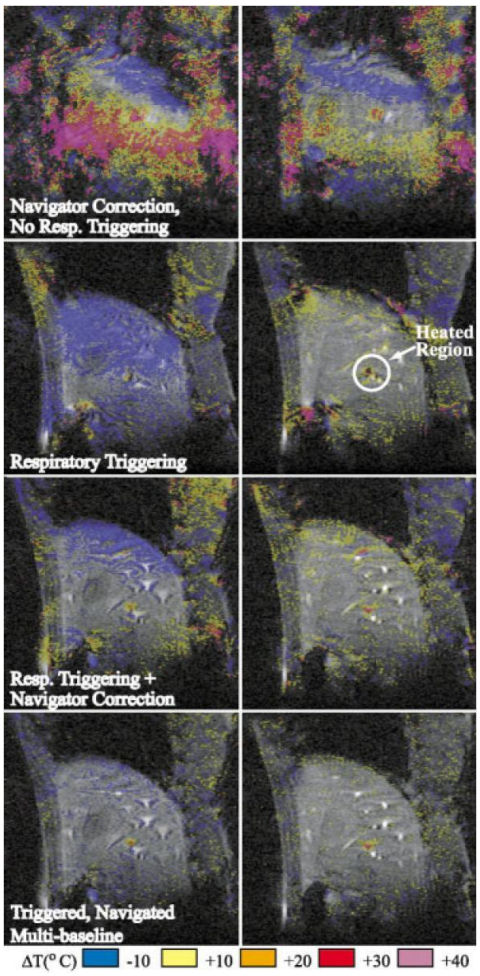

Figure 1. Two time frames during laser heating in the liver of a pig. Reconstructions were performed with no triggering (top row), simple respiratory triggering only (second row), respiratory triggering with navigator phase correction (third row), and the triggered, navigated, multi-baseline method (bottom row). Yellow represents a temperature increase of _10°C over the nominal baseline temperature of 37°C; orange, red, and purple are _20°C, _30°C, and _40°C increases, respectively.

Reproduced with permission from (40).

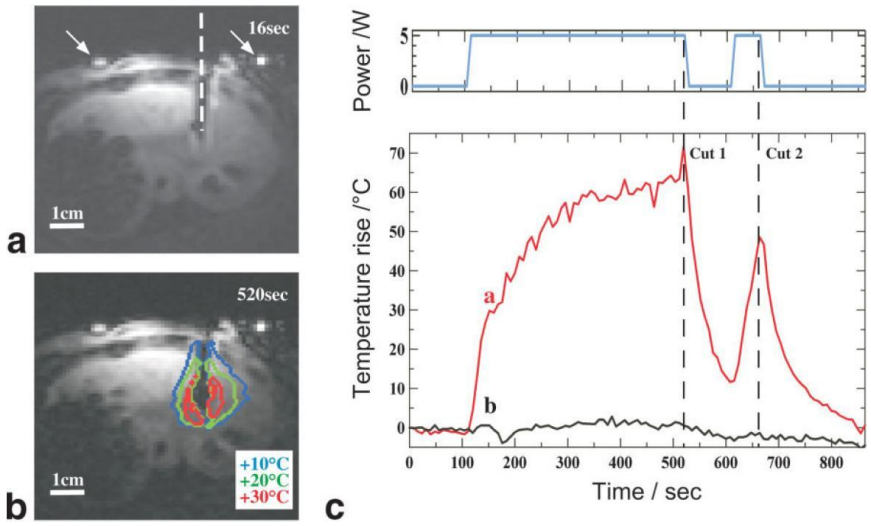

Figure 2. Typical result of a RF ablation with simultaneous temperature MRI. a: Magnitude image obtained 16 seconds after the beginning of MR acquisition and before RF heating. The RF needle is located in the rabbit liver, and its actual size is indicated by the white dashed line. The two bright spots (white arrows) on the two sides of the abdomen of the rabbit are cross sections of the fiducial marker. **b:** Grayscale magnitude image obtained during RF ablation with superimposed increased temperature contours, the levels of which are indicated by color coding (blue = +10°C, green = +20°C, and red = +30°C above starting physiological temperature). **c:** Temporal evolution of temperature for a pixel located at a 2 mm distance from the RF needle (A, in red) and a pixel located at a 20 mm distance (B, in black). The periods of RF power deposition are indicated in blue at the top of c. Two 20% impedance rises occurred, leading to the two cuts of RF power: the first at 520 seconds (cut 1) and the second at 660 seconds (cut 2).

Reproduced with permission from (15).

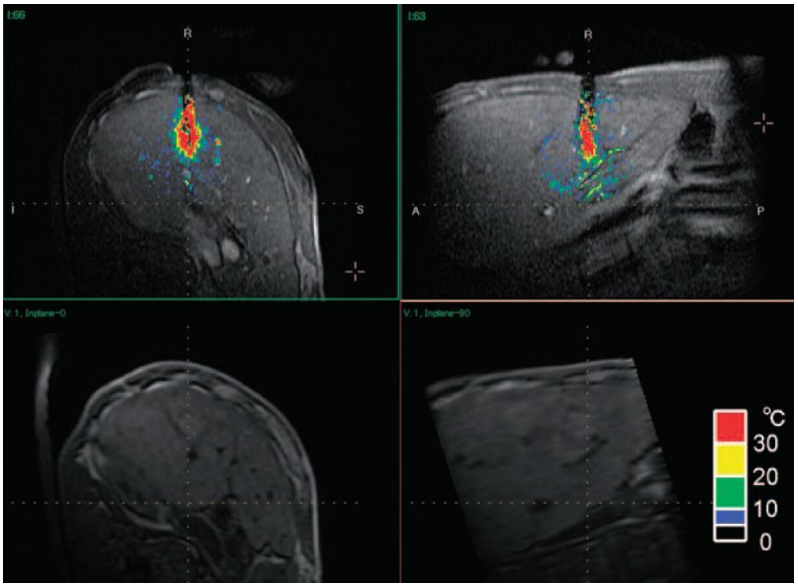

Figure 3. Biplanar temperature maps during the microwave ablation of a liver tumor. The upper two are MR temperature maps and the lower two are reformatted images in the corresponding two perpendicular planes. The color-coded scale on the right, overlaying the magnitude images, indicates the temperature increase.

Reproduced with permission from (52).

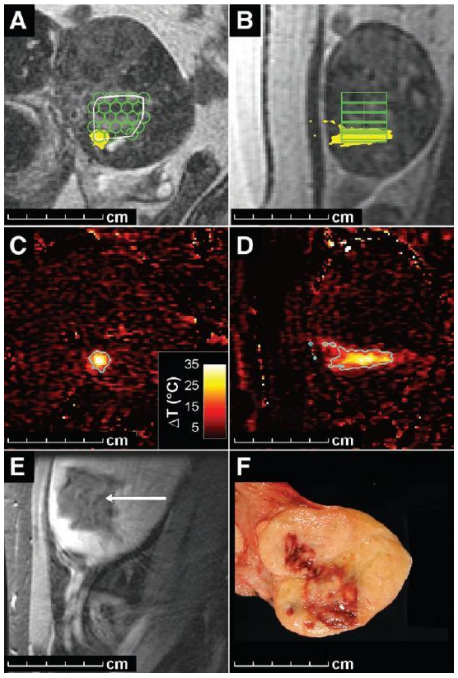

Figure 4. MRgHIFU treatment planning of uterine fibroids, monitoring, progression, and posttreatment followup.

A: Coronal T2-weighted fast SE MR image (4,000/90) was used for treatment planning. Sonication locations and sizes (green lines) were determined with the system planning software from this prescription (and the tissue depth) and were displayed on top of the treatment plan. During treatment, the accumulated thermal dose (yellow area) was displayed on top of treatment planning images. Dose threshold of 240 equivalent minutes at 43°C is displayed.

B: Sagittal T2-weighted MR image (2,500/98) shows treatment plan and area that achieved threshold thermal dose.

C, D: Temperature-sensitive phase-difference fast spoiled gradient-recalled-echo MR images (39.9/19.7) were acquired at peak temperature increase during two sonications. C (coronal view) was acquired perpendicular to the direction of the ultrasound beam, while D (sagittal view) was acquired parallel to the direction of the beam. C and D were used to estimate the thermal dose (blue line) for each sonication.

E, F : Images depict result of treatment. E, Sagittal contrast-enhanced gradient-recalled-echo MR image (245/1.8) was acquired 2 days after ultrasound surgery. Non-enhancing area (arrow) is seen clearly in F, which is a gross pathologic cut specimen that shows the central area of hemorrhagic necrosis.

Reproduced with permission from (3).